



ERNEST ORLANDO LAWRENCE
BERKELEY NATIONAL LABORATORY

Prototype Systems for Measuring Outdoor Air Intake Rates in Rooftop Air Handlers

William J. Fisk
Wanyu R. Chan
Toshifumi Hotchi

Indoor Environment Group
Energy Technologies Area

January 2015

This work is supported by the California Energy Commission Public Interest Energy Research Program, Energy-Related Environmental Research Program, award number PIR-12-031 under US Department of Energy Contract No. DE-AC02-05CH11231.

Disclaimer

This document was prepared as an account of work sponsored by the United States Government. While this document is believed to contain correct information, neither the United States Government nor any agency thereof, nor The Regents of the University of California, nor any of their employees, makes any warranty, express or implied, or assumes any legal responsibility for the accuracy, completeness, or usefulness of any information, apparatus, product, or process disclosed, or represents that its use would not infringe privately owned rights. Reference herein to any specific commercial product, process, or service by its trade name, trademark, manufacturer, or otherwise, does not necessarily constitute or imply its endorsement, recommendation, or favoring by the United States Government or any agency thereof, or The Regents of the University of California. The views and opinions of authors expressed herein do not necessarily state or reflect those of the United States Government or any agency thereof, or The Regents of the University of California.

Ernest Orlando Lawrence Berkeley National Laboratory is an equal opportunity employer

Prototype Systems for Measuring Outdoor Air Intake Rates in Rooftop Air Handlers

William J. Fisk, Wanyu R. Chan, and Tosh Hotchi

Indoor Environment Group
Lawrence Berkeley National Laboratory
Berkeley, CA 94720

January 7, 2015

ABSTRACT

The widespread absence of systems for real-time measurement and feedback control, of minimum outdoor air intake rates in HVAC systems contributes to the poor control of ventilation rates in commercial buildings. Ventilation rates affect building energy consumption and influence occupant health. The project designed fabricated and tested four prototypes of systems for measuring rates of outdoor air intake into roof top air handlers. All prototypes met the $\pm 20\%$ accuracy target at low wind speeds, with all prototypes accurate within approximately $\pm 10\%$ after application of calibration equations. One prototype met the accuracy target without a calibration. With two of four prototype measurement systems, there was no evidence that wind speed or direction affected accuracy; however, winds speeds were generally below usually 3.5 m s^{-1} (12.6 km h^{-1}) and further testing is desirable. The airflow resistance of the prototypes was generally less than 35 Pa at maximum RTU air flow rates. A pressure drop of this magnitude will increase fan energy consumption by approximately 4% . The project did not have resources necessary to estimate costs of mass produced systems. The retail cost of components and materials used to construct prototypes ranged from approximately $\$1,200$ to $\$1,700$. The test data indicate that the basic designs developed in this project, particularly the designs of two of the prototypes, have considerable merit. Further design refinement, testing, and cost analysis would be necessary to fully assess commercial potential. The designs and test results will be communicated to the HVAC manufacturing community.

1.0 Introduction

Higher minimum ventilation rates (MVRs) of outdoor air (OA) usually increase a building's energy consumption and peak power demands (Benne, Griffith et al. 2009, Dutton and Fisk 2014); thus, from an energy perspective MVRs should be as low as possible. However, when MVRs are lowered, indoor air concentrations of pollutants emitted from indoor sources increase. Research has shown that lower ventilation rates (VRs) are associated with decreased satisfaction with indoor air quality (IAQ), increased prevalence rates of acute health symptoms, increased risks of chronic health effects, and reduced work performance (Seppänen, Fisk et al. 1999, Fisk, Black et al. 2011, Sundell, Levin et al. 2011, Parthasarathy, Fisk et al. 2013). The MVRs provided in buildings must strike a balance between the energy benefits and adverse IAQ-related effects of lower VRs. Standards, such as California's Title 24 (California Energy Commission 2013) and Standard 62.1 of the American Society of Heating, Refrigerating, and Air Conditioning Engineers (ASHRAE 2013) specify MVRs for commercial buildings that attempt to strike the correct balance.

Standards alone do not assure maintenance of the desired MVRs. Measurements clearly show that MVRs are poorly controlled in U.S. commercial buildings. In large offices and large stores, MVRs usually exceed requirements; however, some buildings have less ventilation than specified in ASHRAE and California standards (Persily and Gorfain 2008, Siegel, Srebric et al. 2012, Chan, Cohen et al. 2014). In a year-long study of 16 office spaces from three California regions, the estimated average MVR was 15.4 L/s per person, and the median was 14.3 L/s per person, which compare to the required MVR of 7.1 L/s per person in California (Mendell, Eliseeva et al. 2014). Fewer data are available from small and medium offices and stores but the available data are sufficient to confirm poor control of VRs (Bennett, Fisk et al. 2012, Chan, Cohen et al. 2014). In public school buildings in the U.S., VRs often fall far short of minimum requirements (Haverinen-Shaughnessy, Moschandreas et al. 2011, Mendell, Eliseeva et al. 2013).

Several factors likely contribute to the poor control of MVRs. These factors include uncontrolled air leakage through building envelopes, differences between design and actual occupancy (with actual occupancy often lower), and failure to continuously operate heating, ventilating, and air conditioning (HVAC) systems during occupancy. However, poor control of MVRs is also a consequence of the absence, in almost all commercial buildings, of systems for real-time measurement and feedback control, of minimum OA intake rates in HVAC systems.

Accordingly, manufacturers have begun to market technologies for real-time measurement of OA intake rates. In a prior study, three of these technologies were evaluated (Fisk, Faulkner et al. 2005a, Fisk, Faulkner et al. 2005c) and none proved consistently adequate for HVAC systems with economizers, which are very common, particularly in California's mild climates. The causes of poor measurement accuracy, (Fisk, Faulkner et al. 2005b) included low, hard-to-measure, air speeds when minimum outdoor air ventilation is provided as well as complex airflow patterns, sometimes with recirculating eddies, in the outdoor air intake sections of air handlers.

To help overcome the problem of poor control of MVRs, this project has designed and tested prototype measurement systems for OA intake rates in roof-top air handling units (RTUs). The project focused on technologies for RTUs, because RTUs are very common and also because the project is a component of a larger effort to develop an energy retrofit toolkit for small and medium-size commercial buildings which often employ RTUs. One of the toolkit's energy retrofit options is to improve the control of MVRs. However, to implement such a retrofit, a system to measure the OA intake rate is needed.

In practice, systems for measurement of outdoor air intake rates would be used in commissioning to facilitate the initial setting of dampers in outdoor air, supply air and recirculation airstreams and then throughout building operation to maintain OA intake rates at targets, preventing excessive VRs or insufficient ventilation to meet standards. Some examples of applications of measurement systems for OA intake rates follow:

- As supply air flow rates in variable air volume HVAC systems are modulated, OA intake rates will often deviate from the target rates; however, OA intake measurement systems would enable dampers to be adjusted automatically to maintain the targeted MVR.
- The need for ventilation varies with occupancy. MVRs could be adjusted over time as occupancy varies. Advances in occupancy counting systems will facilitate this application.
- The energy costs of ventilation vary as the weather varies and during each day as temperatures and humidity vary. MVRs could be adjusted as the outdoor temperature and humidity, and associated energy costs, of ventilation vary.
- Systems for measuring MVRs will facilitate peak demand response by enabling a controlled temporary reduction in MVRs to reduce peak energy demands and associated high energy costs.
- Systems that measure OA intake rates when the economizer is activated could detect faults in economizer systems. For example, the measurement system would detect when the economizer has a failure and does not increase the VR during mild weather.

2.0 Methods

2.1 Design targets

The project targeted outdoor airflow measurement technologies (OAMTs) that could provide real time (continuous) or high frequency measurements of the minimum outdoor air intake flow rates in RTUs. Many RTUs draw in outdoor air through a hood and an outdoor air damper as illustrated schematically in Figure 1 (A and B). The purpose of the hood is to limit moisture entry into the RTU. The hoods typically bolt to the RTU enclosure. The project targeted OAMTs that either replaced the existing hood or that could be inserted between the hood and the RTU cabinet as shown in Figure 1 (C and D), making the technologies applicable for both new RTUs and retrofits.

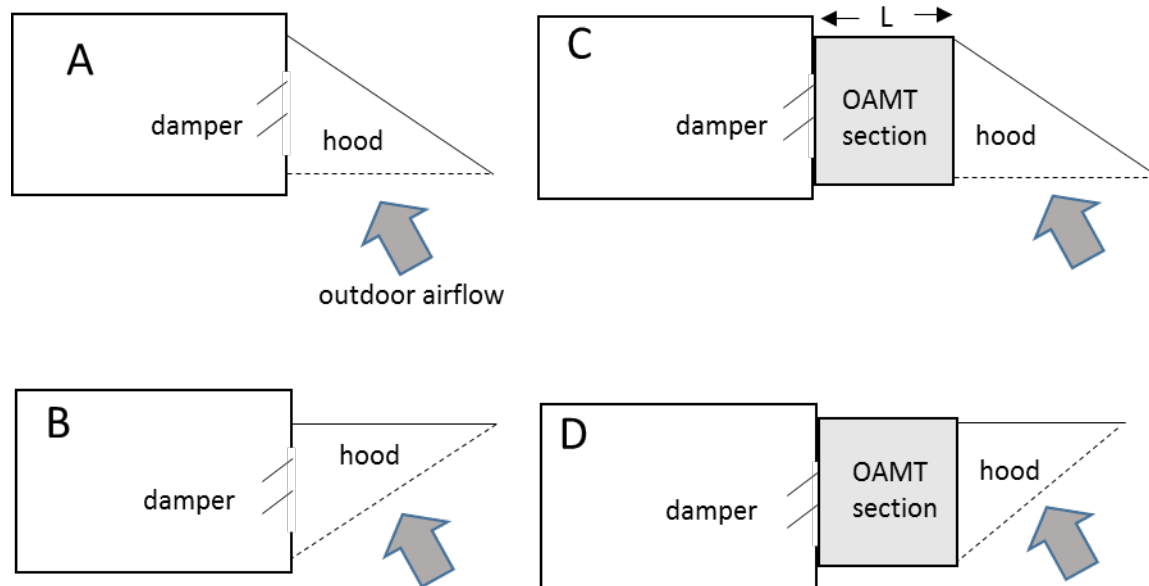


Figure 1. Schematic showing typical configurations of outdoor air intake hoods and outdoor air dampers in RTUs (A and B) and target locations for OAMTs (C and D).

For illustrative purposes the size of the intake hoods and OAMTs are exaggerated relative to the size of the RTU cabinets. The vertical sides of the hoods are closed; thus, outdoor air enters only by passing through the planes of the dotted lines, representing coarse wire mesh screens.

The prototype OAMTs were designed for use in RTUs with outdoor air economizer systems. Economizers are hardware and control systems that increase the OA VRs above MVRs during mild weather when providing an increased amount of outdoor air reduces the energy needed for space cooling. While many existing small and medium-size RTUs lack economizers, they are now required by California's Title 24 Standard in all HVAC systems with a cooling capacity above 15.8 kW (California Energy Commission 2013); thus, the future stock of RTUs is expected to be dominated by RTUs with economizers. Economizers make measurement of outdoor airflow rates more challenging. The OA intake systems must be sized to accommodate the high outdoor air flow rates during economizer activation. The air speeds in OA intake systems are constrained in order to limit moisture entry into HVAC systems, as well as to limit airflow resistance. When minimum VRs are provided, OA flow rates will often be 10% to 20% of the maximum OA flow rate during economizer activation, leading to very low air speeds in the streams of incoming OA. It can be very challenging to accurately measure the resulting low air speeds using the pressure-based velocity measurement methods probes that are most common in HVAC systems (Fisk, Faulkner et al. 2005b).

Measurements of OA intake rates are only necessary during periods when the MVR is provided. In HVAC systems without economizers, the MVR is provided at all times. In HVAC systems with economizers, the MVR is provided when weather is hot or cold and a higher VR would increase energy costs. During mild weather, increased ventilation often saves energy and

the economizer control system controls the VR. Thus, OAMTs that measure OA intake rates only when the economizer is deactivated were considered acceptable.

The airflow resistance of an OAMT will generally increase the fan energy consumption of the RTU, thus, it is desirable to minimize the airflow resistance. The target was an increase in pressure drop for an OA intake system incorporating an OAMT of 35 Pa or less. The total airflow resistance of components of a variable air volume RTU and its air distribution system is on the order of 1,000 Pa and fan energy use will vary approximately in direct proportion to total airflow resistance, so a 35 Pa pressure drop will increase fan energy use by roughly 4%. As another point of reference, particle filters for commercial buildings are often replaced when pressure drops exceed approximately 250 Pa (Fisk, Faulkner et al. 2002, Arnold, Matela et al. 2005).

The accuracy target for the measurement of OA flow rate was $\pm 20\%$. Changes in building energy consumption and IAQ associated with $\pm 20\%$ or smaller errors in OA flow rate will be modest (Dutton and Fisk 2014) and OAMT costs were expected to increase as the accuracy requirement is tightened.

In most RTU installations, there is much free space surrounding the RTU, placing little practical constraint on the size of an OAMT. However, some installations have panels that serve as visual screens surrounding RTUs. A rigid target was not established for horizontal length (dimension L in Figure 1) of the OAMT; however, there was a general goal of maintaining horizontal length as small as practicable.

The design objective was to maintain the expected OAMT cost as low as possible, ideally less than 20% of the cost of a RTU retrofit. Costs of RTU retrofits (Pacific Northwest National Laboratory 2014) are estimated to be \$250 to \$430 per kW of cooling capacity (\$900 to \$1500 per ton). Thus an intermediate size 35 kW (10 ton) RTU retrofit is expected to cost \$9000 to \$15000 and a 20% target corresponds to \$1800 to \$3000. The cost of an OAMT will not change linearly with the size of the RTU because the cost of some of the components, such as sensors, will not be highly affected by RTU size. Consequently, it will be more difficult to produce practical cost OAMTs for small RTUs.

2.2 Design process

The designs concepts were based on the results of prior research (Fisk, Faulkner et al. 2005b) with the following findings:

- Air velocity measurement systems that rely on sensing of velocity pressure to determine air speeds will not be sufficiently accurate in systems with economizers unless the cross sectional area of the airflow paths are reduced when the economizer is deactivated.
- The air flow patterns within the OA intake sections of HVAC systems can be highly complex because of changes in air direction as a result of OA flow through air intake hoods, louvers, dampers, and other components. Air flow rate measurements based on

deployment of multiple airspeed sensors in locations with complex airflow patterns and unknown airflow directions will often be highly inaccurate.

- Accurate measurement of OA intake rates will be facilitated by
 - conditioning of the airflow, so that the direction of airflow at the location of air velocity sensors is uniform and known, and
 - use of air velocity sensors that are accurate at the airspeeds encountered when MVRs are provided.

Using these design concepts as a base, various configurations and hardware systems for OAMTs were considered and evaluated using standard engineering methods to predict air velocities, airstream pressure drops, and measurement accuracy. Costs were also roughly estimated. To support these analyses, data were collected on the specifications, accuracy, and cost of electronic air velocity sensors, pressure-based velocity probes, pressure transducers, and hardware potentially suitable for this application. These data were used in the evaluation of prototype designs. The choice of velocity sensors was constrained to sensors suitable for outdoor air intake locations where temperature and humidity can vary over a large range. An iterative process was employed, at time obtaining feedback from a prominent HVAC design firm, eventually resulting in the designs of four prototype OAMTs. Three of the prototypes, designated OAMT1a, OAMT1b, and OAMT1c, were intended for measurement of OA flow rates during periods of minimum OA supply as well as during periods of economizer activation. A fourth prototype, designated OAMT2, was designed as a lower cost product that only measured OA flow rates during periods of minimum OA supply.

2.3 Evaluation Facility

The temperature and humidity of OA entering RTUs, and other types of HVAC systems, will vary depending on the local weather conditions. In periods with precipitation or fog, small suspended water droplets may be carried into the RTU by the OA, possibly affecting sensors. Winds, with temporal changes in both speed and direction, may influence the air speeds and static pressures at the OA intake. Because it is very challenging to reproduce these conditions in a laboratory, the research team opted to test the prototypes using a unique test system located on the rooftop of a building on the Lawrence Berkeley National Laboratory (LBNL) campus. The building is located on a slope with the rooftop approximately 10 m above grade on the downhill side of the building. Figure 2 schematically illustrates the main components of the test system.

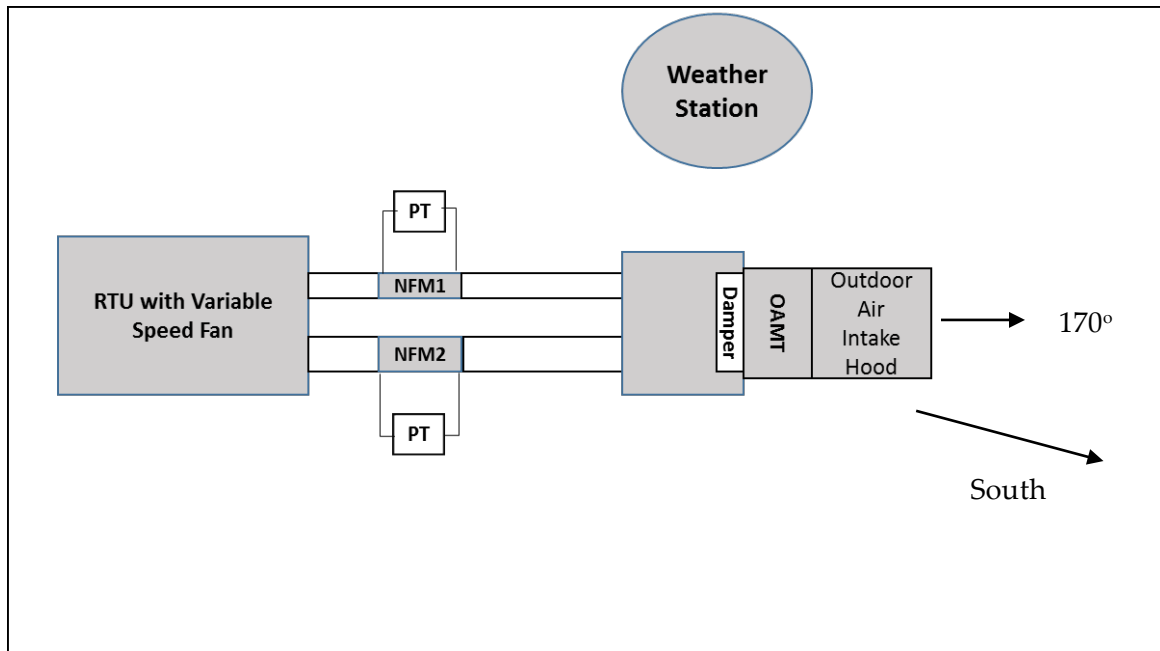


Figure 2.Figure 2: Schematic top view of main features the evaluation system located on a horizontal building rooftop.

NFM1 and NFM2 are different size nozzle flow meters. PT is a pressure transducer.

The evaluation system has a variable speed fan controlled by a variable frequency drive and the design maximum system flow is approximately $1,200 \text{ L s}^{-1}$, although maximum flow rates in practice were approximately $1,000 \text{ L s}^{-1}$. This design peak flow rate is typical of a RTU with a 22kW (6.25 ton) of refrigeration capacity. While 22 kW is a small RTU, the prototype OAMTs could easily be scaled to a larger size. Immediately downstream of the OAMT is a cabinet housing an opposed-blade damper; thus, the downstream hardware in the test system is like the cabinet and OA intake damper of a typical RTU.

The major testing challenge was to obtain a highly accurate reference measurement of the OA flow rate to which the air flow rate indicated by the OAMT could be compared, while locating the OAMT outdoors on a building rooftop. For the reference measurements of OA flow rates, the evaluation system includes a pair of different size nozzle airflow meters with upstream honeycomb airflow straighteners (NFM1 and NFM2), connected to research-grade pressure transducers (PTs). Sections of straight pipe upstream and downstream of the nozzle flow meters are provided in accordance with the manufacturer's specifications. Plates can be installed to prevent airflow through either nozzle flow meter, so that airflow can be measured using either the smaller, larger, or both nozzle flow meters, enabling the flow rates through the airflow meters to be maintained in the range that produces a pressure signal of sufficient magnitude for accurate measurement. A weather station located 3 m above the rooftop, measures wind speed, wind direction, temperature, and humidity. Table 1 provides summary information on the key instruments.

Table 1. Key instrumentation in evaluation system.

Item	Make and Model	Range	Purpose	Manufacturer's rated accuracy	Calibration or Performance Check
Small nozzle flow meter	Thermo-Brandt Instruments NZP-1031 6 inch	0.07 – 0.24 m ³ s ⁻¹	Reference measurement of outdoor air flow rate	±0.5%	Compared to Pitot-static tube traverse in long straight duct
Large nozzle flow meter	Thermo-Brandt Instruments NZP-1031 12 inch	0.19 – 0.67 m ³ s ⁻¹	Reference measurement of outdoor air flow rate	±0.5%	Compared to Pitot-static tube traverse in long straight duct
Multi-channel pressure transducer	Energy Conservatory APT-3-8	0 – 300 Pa and 0- 1000 Pa	Measure pressure signals of nozzle flow meters Measure airflow resistance of OAMT	± 1% of reading	Factory re-calibration immediately before deployment plus cross check with other instruments
Hot wire anemometer	TSI 9545	0 – 30 m s ⁻¹	Check velocity profile in plane of the OAMT's airflow sensors	± 3% or ± 0.15 m s ⁻¹	Factory calibration
Wind speed Wind direction Outdoor temperature	Davis Instruments Vantage Vue Wireless Weather Station	3-241 km/h 0 – 360° -40 – 65 °C	Characterize outdoor weather conditions	± 3 km/h ± 3° ± 0.5 °C	Factory calibration
Air temperature	Precision Thermistor Energy Conservatory APT-3-8	-40 – 100 °C	Characterize temperature of air in OAMT	± 0.25 °C (0 – 75 °C)	Factory Calibration

The rate of airflow through the nozzle flow meters was determined using the following equation

$$F = A_e \sqrt{2 \Delta P / \rho} \quad (1)$$

where F is the actual flow rate in m³ s⁻¹, ρ is the density of the air in kg m⁻³, ΔP is the pressure signal of the nozzle flow meter in Pa, A_e is the effective area of the nozzle in m², provided by the

manufacturer. The values of A_e are 0.00857 m² and 0.0353 m² for the small and large nozzle flow meter, respectively. Air density was calculated from

$$\rho = \frac{P_{atm}}{R T} e^{(-9.8 H)/(R T)} \quad (2)$$

where P_{atm} is the atmospheric pressure, ρ is the density (kg m⁻³), R is the gas constant for air (J kg⁻¹ K⁻¹), T is the temperature in degrees Kelvin, and H is the altitude (m).

The key factors leading to uncertainty in the reference measurements of OA flow rates (values of F in equation 1) are the uncertainty in the measurement of the pressure signal ΔP and in the effective area of the nozzle. The pressure signal of the pressure transducer connected to the nozzle airflow meters was maintained above 16 Pa. While the rated accuracy of the pressure transducer is 1% of the measured value, 0.16 Pa at 16 Pa, given the uncertainty in the process for checking the calibration of the pressure transducer, a higher pressure measurement uncertainty of ± 1.5 Pa is assumed, resulting in an associated uncertainty of $\pm 5\%$ for the reference measurements of OA flow rate. The nozzle manufacturer lists an uncertainty of $\pm 0.5\%$, although the basis for this number is unclear. The uncertainty in air density will be negligible. Adding these uncertainty components in quadrature leads to a total estimated uncertainty of 5% for the reference measurements of OA flow rates.

2.3 Evaluation protocols

To evaluate the OAMTs, they were installed in the roof-top evaluation system and the OA flow rates indicated by the OAMTs were compared to the reference OA flow rates determined from one of the nozzle flow meters. The smaller nozzle flow meter (NFM1) was used for flow rates of 0.08 to 0.3 m³ s⁻¹, and the larger NFM (NFM2) used for higher flow rates. A plate was installed to prevent airflow through NFM1 or NFM2 when it was not used.

Data were collected with the OA damper located downstream of the OAMT either 25% or 75% open, based on angle of rotation of the damper's shaft. Also, the location of air velocity probes, relative to the location of the damper was varied.

Two types of evaluations were performed. First, for each hardware configuration, (e.g., damper opening and velocity probe location) the rate of OA flow was stepped through the full range of interest by varying the fan speed, while maintaining each flow rate constant for approximately 60 minutes. These tests were performed when wind speeds were low, usually below 2 m s⁻¹ (7.2 km h⁻¹). Parts of the data were used to generate system calibration curves and additional data were used to check measurement accuracy after application of the calibration curves. The system was also operated for periods of days to weeks with a fixed hardware configuration and OA flow rate while wind speed, wind direction, and outdoor temperature and humidity varied naturally. The primary purpose of these longer-term experiments was to enable a determination of the extent to which wind conditions affected the accuracy of the OAMTs.

3.0 Results

3.1 Measurement System Designs

3.1.1 Design of OAMT1a and OAMT1b

Figure 3 illustrates the basic design of OAMT1a and OAMT1b and how they connect to a RTU. The left-most section of the figure shows the OA inlet damper and cabinet of the RTU, which is not part of the OAMT units. The incoming OA passes in turn through an air inlet hood with turning vanes, a honeycomb airflow straightener, and then a short section of duct containing velocity probes. Dimensions are provided for the system fabricated but would be modified depending on the size of the RTU. The existing inlet hood was replaced by a hood with turning vanes and a curved top to eliminate abrupt changes in airflow direction. The honeycomb straightener has 0.02 m hexagonal cells that are 0.15 m deep in the direction of airflow, resulting in a ratio of length to hydraulic diameter of 7.9. The honeycomb module is slightly larger in cross section than the airflow passages entering or exiting the honeycomb media so that there is no obstruction of the airflow, i.e., the frame housing the honeycomb is not within the airflow path. The air velocity through the honeycomb media and duct section housing the velocity probes ranges from approximately 0.42 m s^{-1} at 10% OA supply (when the OA flow rate is 10% of the supply flow rate) to 4.2 m s^{-1} at 100% outdoor air supply. At the low end of this velocity range, pressure based velocity probes will not be accurate because the pressure signal is too small for accurate measurement using practical pressure transducers. The electronic velocity probes selected (Table 2) are ones marketed specifically for measuring OA intake flow rates. They have a range of 0 to 25.4 m s^{-1} , are temperature compensated, and are advertised for 0 to 99% relative humidity. OAMT1a contains a single centrally-located probe containing four velocity sensors and extends the 0.79 m width of the OAMT. OAMT1b contains two probes each with two velocity sensors, with probes extending the width of the OAMT. In each case, the probe or probes are used together with transmitters that provide one air velocity that equals the average velocity at all sensors. The prototypes contained provisions, not shown in Figure 3, for installation of the velocity probes various distances from the outlet of the honeycomb airflow straightener, which would not be a feature of a final design.

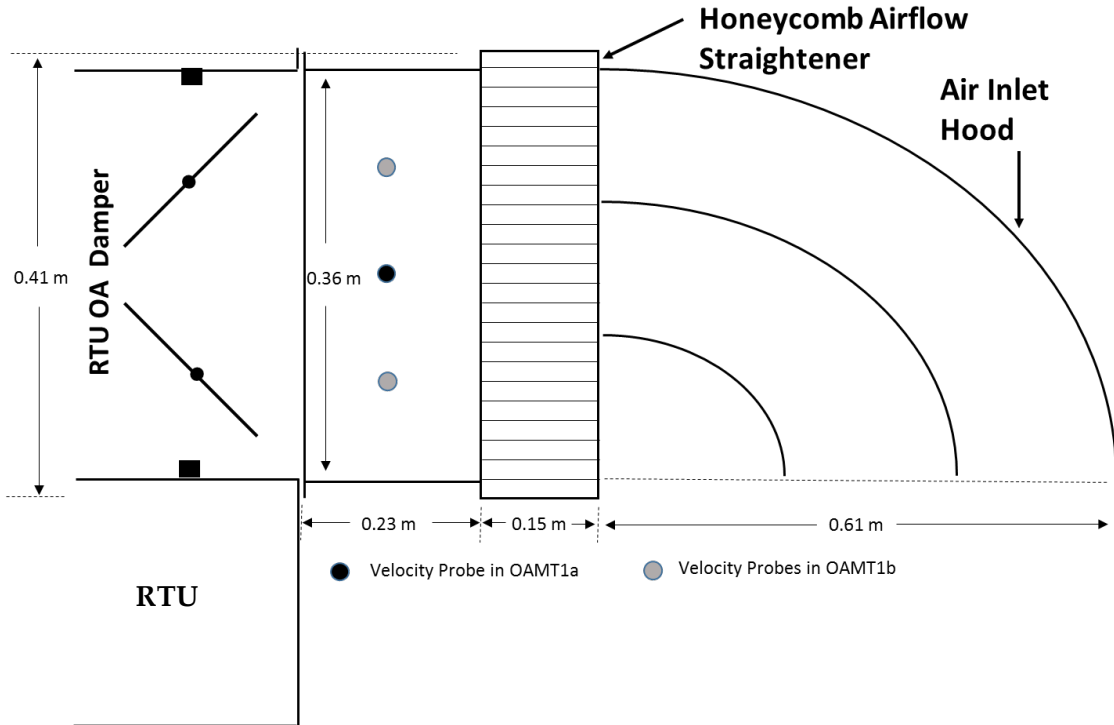


Figure 3: Schematic of cross section of OAMT1a and OAMT1b.

The honeycomb airflow straightener is the major source of airflow resistance of OAMT1a and OAMT1b, relative to a traditional OA intake hood. Extrapolation from data provided by the honeycomb manufacturer for honeycomb media 2.5 and 5 cm deep, yielded an estimated pressure drop ranging from 0.5 to 4 Pa over the full range of air velocity of 0.42 to 4.05 m s⁻¹. Engineering calculations yielded an estimated range of pressure drop of 1.3 to 7.6 Pa for the same range of flow rates.

The most costly components of OAMT1a and OAMT1b are the electronic velocity probes and associated electronics. The retail cost of the single probe plus transmitter of OAMT1a was \$978. The dual-probe system used in OAMT1b cost \$1,323. The honeycomb media cost \$90. Probes from other vendors were evaluated, but their cost and performance specifications were not considered superior. The cost of materials to fabricate the sheet metal components in shops at Lawrence Berkeley National Laboratory was \$250. Thus, the total retail cost of components and materials was \$1,318 for OAMT1a and \$1,663 for OAMT1b. The sheet metal fabrication cost for the prototype was \$4,350; however, mass production costs for materials and labor would be much less.

Low cost air velocity sensors are becoming available and such sensors might reduce the costs of OAMTs. For example, Omron markets temperature compensated sensors with ranges of 0-1, 0-4, and 0-10 m s⁻¹ and a rated accuracy of $\pm 5\%$. They incorporate a design for preventing sensor

contamination by dust. Their retail cost is \$65. They are designed for an operating temperature range of -10 to 60 °C and a relative humidity range of 0% to 85%. It is not clear how well these sensors would perform over the long term at the OA intake of a RTU where relative humidity can often exceed 85% and temperatures fall below -10 °C. Sensors that became inaccurate when humidity exceeds 85% would still be usable in many climates, since it is not critical to measure OA flow rates at all times. However, sensors damaged by high humidity or low temperature will not be usable in OAMTs. Due to budget and time limitations, tests of a version of OAMT1 with the lower cost Omron sensors were not performed

Table 2: Electronic velocity probes* employed in OAMT1a, OAMT1b, and OAMT1c.

System	Manufacturer and Model	Number of Probes Used	Number of Velocity Sensors per Probe	Manufacturer's Range	Manufacturer's Accuracy
OAMT1a And OAMT1c	Ebtron HTA104PB	1	4	0 – 25.4 m s ⁻¹ -30 – 71 °C 0 – 99% RH	± 2% of reading ± 0.25% repeatability
OAMT1b	Ebtron GT 116 PC	2	3	0 – 25.4 m s ⁻¹ -30 – 71 °C 0 – 99% RH	± 2% of reading ± 0.25% repeatability

*Probes come with transmitters with a 4 to 20 mA output signals that were converted to a voltages.

The airflow rate measured by OAMT1a and OAMT1b, without incorporation of any calibration factors, was the product of the average velocity indicated by the probe(s) and the cross sectional area of the airflow path, which equals the cross sectional area of the duct holding the probe(s) minus the cross sectional area of the probe(s). Probes were 0.028 m in diameter and the inserted length of probes, equal to the horizontal width of the duct, was 0.794 m. Thus, each probe blocked 0.022 m² of the 0.292 m² duct. Consequently the airflow rates of OAMT1a (with one velocity probe) and OAMT1b (with two velocity probes), before adjustments based on comparisons to the reference airflow meters were applied, were calculated as follows:

$$F_{1a} = 0.270 V_{1a} \quad (3)$$

$$F_{1b} = 0.248 V_{1b} \quad (4)$$

where F_{1a} (m³ s⁻¹) is the flow rate indicated by OAMT1a and F_{1b} (m³ s⁻¹) is the flow rate indicated by OAMT1b, V_{1a} and V_{1b} (m s⁻¹) are the air velocities indicated by the probes in OAMT1a and OAMT1b, respectively. All volumetric air flow rates are actual values, at the density encountered.

Air velocities were determined from the voltage output by the transmitter components of the probe systems, per instruction in product literature. For OAMT1a, the velocity (m s^{-1}) is

$$V_{1a} = 3124 E_{1a} - 1247 \quad (5)$$

where E_{1a} is the output voltage. For OAMT1b the velocity (m s^{-1}) is

$$V_{1b} = 3138 E_{1b} - 1256 \quad (6)$$

where E_{1b} is the output voltage.

3.1.2 Design of OAMT1c

Late in the project term, OAMT1c was designed and fabricated. Time and funding constraints limited the period of testing of this system. The design, depicted in Figure 4, is similar to the design of OAMT1a, with the same single electronic velocity probe (Ebtron HTA104PB) containing four velocity sensors centered downstream of an airflow straightener. However, in place of the honeycomb straightener of OAMT1a, a square channel airflow straightener is used in OAMT1c. In a mass-produced OAMT1c, the square tube straightener would be fabricated from cast aluminum or a type of plastic that meets flame spread and smoke density requirements, with a channel wall thickness on the order of 1 mm to maintain strength and rigidity. However, to reduce fabrication costs in the prototype, the square tube airflow straightener was a stack of thin-walled (0.38 mm thick) square plastic tubes, each tube 0.17 m long. To reduce costs of a mass produced product, OAMT1c also employed a simple standard air intake hood, without the turning vanes that are present in the intake hood of OAMT1a and OAMT1b.

An advantage of a square channel airflow straightener, relative a honeycomb straightener, is that that the square (or rectangular) channel straightener can be designed to fit into a rectangular sheet metal duct without having partial airflow channels at the perimeter. In contrast, when a honeycomb straightener is fit into a rectangular duct, the honeycomb media must be cut in a manner that leaves many partial cells at the perimeter. The resulting thin metal strips of aluminum honeycomb media at the perimeter of a honeycomb straightener are very easily bent. To produce a relatively undisturbed path for airflow at the perimeter, a separate module containing a slightly oversize section of honeycomb was required. Thus, OAMT1a and OAMT1b, with honeycomb straighteners, have three modules that are bolted together in series (hood, straightener, and probe module), while OAMT1c has two modules (hood and straightener plus probe module).

The retail cost for the velocity probe and associated transmitter of OAMT1c is \$978 and the retail cost of sheet metal was approximately \$170. The materials cost for the airflow straightener, constructed from square plastic tubes was minimal. Allowing \$150 for metal airflow straighteners, the total retail component cost was \$1,298. The labor cost for sheet metal fabrication of the prototype was \$2,000. Mass production costs for materials and labor would likely be much lower.

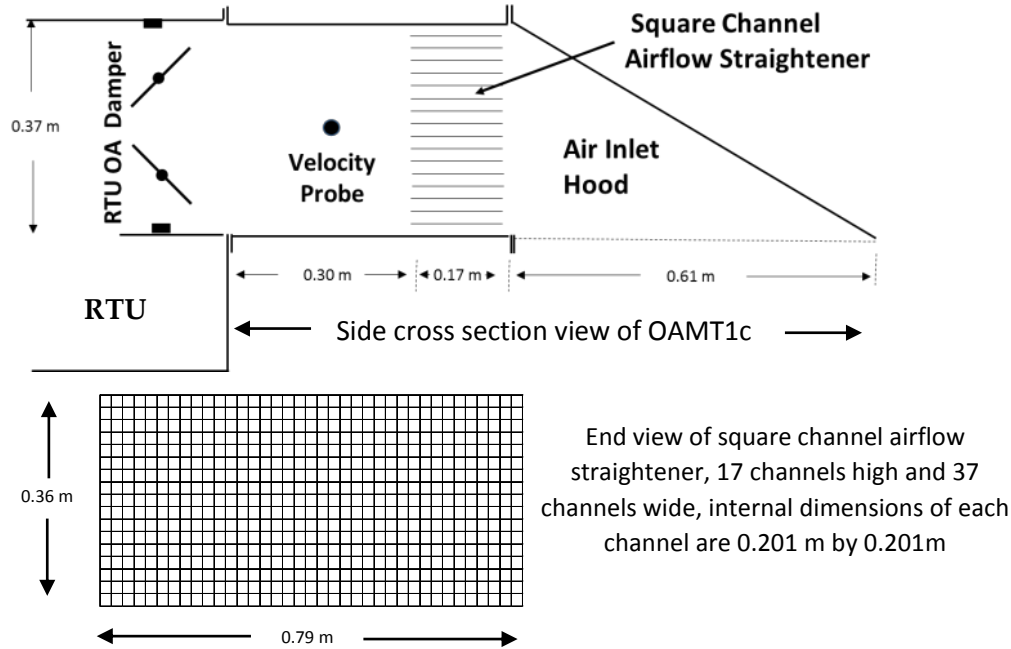


Figure 4. Schematic of OAMT1c.

The airflow rate measured by OAMT1c without incorporation of any calibration factors, was the product of the average velocity indicated by the probe and the cross sectional area of the airflow path, which equals the cross sectional area of the duct holding the probe (0.290 m^2) minus the cross sectional area of the probe (0.022 m^2). The resulting equation is

$$F_{1c} = 0.268 V_{1c} \quad (7)$$

where F_{1c} ($\text{m}^3 \text{ s}^{-1}$) is the flow rate indicated by OAMT1c in cubic meters per second and V_{1c} (m s^{-1}) is the air velocity indicated by the probe in OAMT1c. Air velocity was determined from probe outlet velocity as indicated in equation 3.

3.1.3 Design of OAMT2

Figure 5 illustrates the basic design of OAMT2. This system was designed to measure OA flow rates only when minimum OA is provided by the RTU, i.e., when the economizer is deactivated. The system contains a damper and actuator that closes the damper when minimum OA is provided, causing all OA to flow through the OA inlets located above the damper. The OA inlets are short sections of rectangular duct containing airflow straighteners followed by

typical low-cost pressure-based velocity probes. With the damper closed, the velocity of the air at the probes is maintained sufficiently high for accurate measurement with the pressure transducers used in HVAC control systems. The system was designed to maintain pressure signals between 6 and 25 Pa, for use with a pressure transducer that has a 0 – 25 Pa range, and to measure minimum OA flow rates that are 6% to 30% of the total RTU supply air flow rate. Blockage plates can be installed to block airflow through one or two of the OA inlets and maintain pressure signals in the desired range. With all three OA inlets open, measurable OA flow rates are 16% to 30% of total supply flow. With two and one OA inlets open the corresponding ranges are 10%-20% and 6% to 10%, respectively. In usual practice, minimum OA flow rates are unchanged for years, or even for the life of the RTU, so that addition and removal of blockage plates will occur infrequently. A single pressure transducer measures the average pressure signal from all velocity probes. When an OA inlet is blocked, valves are used to disconnect the corresponding velocity probe from the pressure transducer.

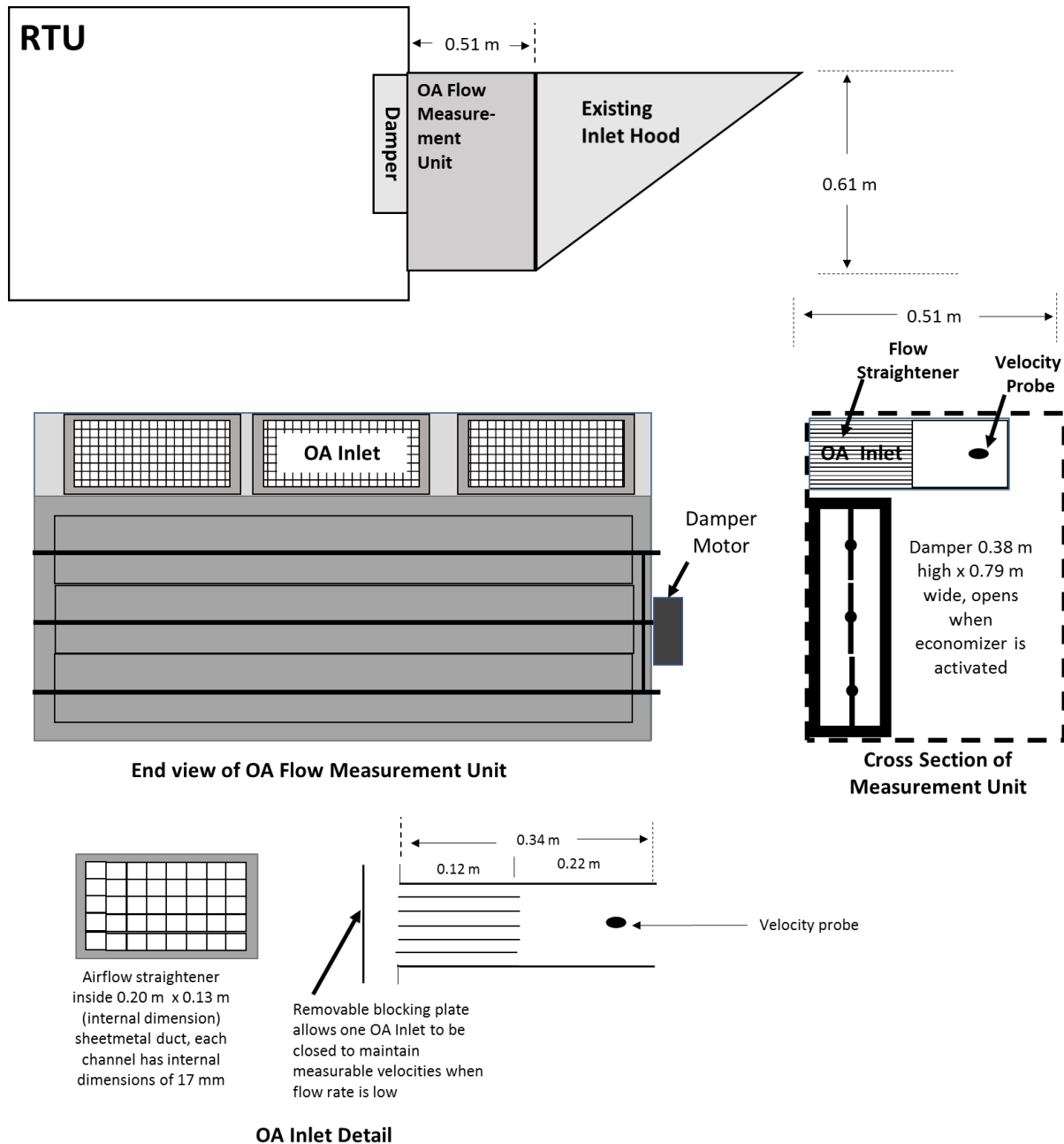


Figure 5. Schematic of OAMT2. The pressure transducer and tubing connecting the transducer to velocity probes is not shown.

Table 3 describes key components in OAMT2. Extrapolating from manufacturer's data, the rate of leakage through the damper when closed, with the maximum expected pressure difference across the damper of 30 Pa, was estimated to be $0.001 \text{ m}^3 \text{ s}^{-1}$ which is approximately 0.3% of the OA flow rate at that condition; thus, leakage is expected to be a negligible source of error.

Table 3. Key components of OAMT2

Component	Manufacturer and Model	Description	Retail cost (\$ US)
Damper	Ruskin CD 36, nominal 0.79 m wide by 0.38 m high	Low leakage damper	\$200
Damper motor	Belimo AF 24	Fully opens or fully closes damper based on the signal provided to the economizer of the RTU	\$200
Velocity Probe	Dwyer PAFS 1004	Probe with 19.6 cm insertion depth, and three sensing points, K factor of 1.46	\$10.5 each, 3 required for total cost of \$31.5
Pressure transducer	Setra 264	0 – 25 Pa range, Rated accuracy of $\pm 0.25\%$ of full scale equal to ± 0.06 Pa	\$532
Airflow straightener	Not applicable. For prototype, the straighteners were printed with a 3-D printer, mass produced versions would most likely be cast aluminum	77 (17 mm by 17 mm internal dimension) air flow channels (11 channels wide and 7 channels high) with 1 mm thick walls	Not available

The airflow straighteners in the prototype were fabricated with a three-dimensional printer. Mass produced straighteners would be fabricated from cast aluminum or a type of plastic that meets flame spread and smoke density requirements, with a channel wall thickness on the order of 1 mm to maintain strength and rigidity.

OAMT2 avoids the use of a honeycomb airflow straightener, incorporated in OAMT1a and OAMT1b. The honeycomb straightener is fragile (easily bent or distorted) and difficult to install in a rectangular duct, as discussed previously. A disadvantage of OAMT2 is the need to tap into the wiring providing a signal to the economizer of the RTU (a feature not implemented in the prototype), although the anticipated cost is low using a connector that is inserted in-line with the connector to the economizer’s damper motor.

An advantage of the OAMT2 design relative to OAMT1 is that the retail cost of the velocity probes plus pressure transducer is \$560, which compares to the retail cost of velocity probes plus transmitters in OAMT1 of \$978 to \$1,323. Also, the reliance on the existing OA intake hood

with OAMT2 reduces costs relative to OAMT1a and OAMT1b which incorporates a new hood, with turning vanes. Also, the simpler sheet metal elements of OAMT2, relative to OAMT1, will reduce costs. These savings are partially offset by the cost of the damper plus damper motor of OAMT2, \$400 retail. If \$150 is assumed as total retail cost of the airflow straighteners and \$75 is assumed for sheet metal, the total retail cost of components of OAMT2 is approximately \$1,185, not including the anticipated minor cost of wiring and a connector needed to access the economizer control signal and use it to open and close the damper of OAMT1c. The labor cost for fabricating the sheet metal of the OAMT1c prototype was \$2,000. Mass production costs for materials and labor would likely be much lower.

The rated accuracy of the Setra pressure transducer used in OAMT is ± 0.16 Pa and the design pressure signal is 6 Pa to 25 Pa. With this accuracy specification, since air flow rate is proportion to the square root of the pressure signal, the uncertainty on OA flow rate due to uncertainties in pressure measurement is 1% to 5%. A larger, and probably more realistic, 0.5 Pa uncertainty in pressure measurement leads to a 4% to 17% uncertainty in OA flow rate.

Using standard engineering calculation methods, the pressure drop of air flowing through the OA inlets during periods of minimum OA flow was estimated to range from 11 to 29 Pa. During periods of economizer activation, the open damper plus OA inlets pose an airflow resistance, relative to a system without an OAMT. Using data from the damper manufacturer, this pressure drop was estimated to be less than 10 Pa.

The airflow rate measured by OAMT2, without incorporation of any calibration factors, was calculated from equation 8

$$F_2 = \sum_1^n (A_{inlet} - A_{probe}) V_2 \quad (8)$$

where F_2 ($\text{m}^3 \text{s}^{-1}$) is the airflow rate, n is the number of open air inlets ranging from 1 to 3, A_{inlet} equals the cross sectional area of an inlet (0.0253 m^2), A_{probe} is the area by which a probe obstructs an inlet (0.0015 m^2), and V_2 (m s^{-1}) is the air velocity. Equation 9 is used to calculate air velocity

$$V_2 = \sqrt{\Delta P / ((1.46) (0.5) (\rho))} \quad (9)$$

where ΔP is the pressure signal from the velocity probe(s), 1.46 is the probe K factor provided by the manufacturer, and ρ is the air density.

3.2 Measurement System Performance

3.2.1 OAMT1a

Figure 6 shows results of tests of OAMT1a with the velocity probe located in upstream and downstream locations in the left and right panels, respectively. When at the upstream location, the probe was 6.4 cm downstream of outlet of the airflow straightener and 16.5 cm upstream of the axis of rotation of the damper blades. When at the downstream location, the probe was 16.5 cm downstream of outlet of the airflow straightener and 6.4 cm upstream of the axis of rotation

of the damper blades. Each data point represents a 20 to 140 minute (normally 60 minute) average value, and the error bars indicate standard deviations of one-minute data points. Data from tests with the downstream damper both 25% open and 75% open were combined, as there was no discernable effect of the degree of damper opening. The shaded sections of the plots correspond to flow rates less than 8% of the system design flow rate, which are less common in practice.

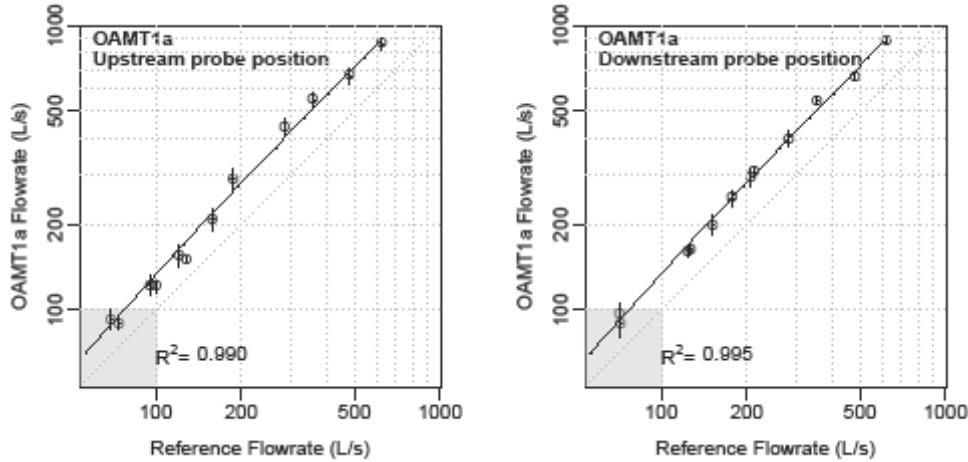


Figure 6. Results of tests of OAMT1a when wind speed are low.

Without application of any calibration factor, the flow rate indicated by OAMT1a is consistently about 40% higher than the reference airflow rate. The corrected flow rates from OAMT1a, with the probe in the upstream position can be calculated from the following equation

$$\text{Corrected } F_{1a} = 0.690 F_{1a} + 8.3 \quad (10)$$

With the probe in the downstream position, the corresponding equation is essentially the same

$$\text{Corrected } F_{1a} = 0.688 F_{1a} + 8.0 \quad (11)$$

The values of R^2 for the linear fits in equations 10 and 11 are 0.990 and 0.995.

To indicate measurement accuracy using equations 10 and 11, and analogous equations to follow for OAMT1b, the equations were applied to data that were not used not for generation of the equations. The resulting air flow rates are compared to reference values of airflow rate on Figure 7. Nearly all the data points fall within the $\pm 10\%$ confidence band indicating that errors are generally less than 10%. Again, the shaded section of the plot corresponds to flow rates less than 8% of the system design flow rate, which are less common in practice.

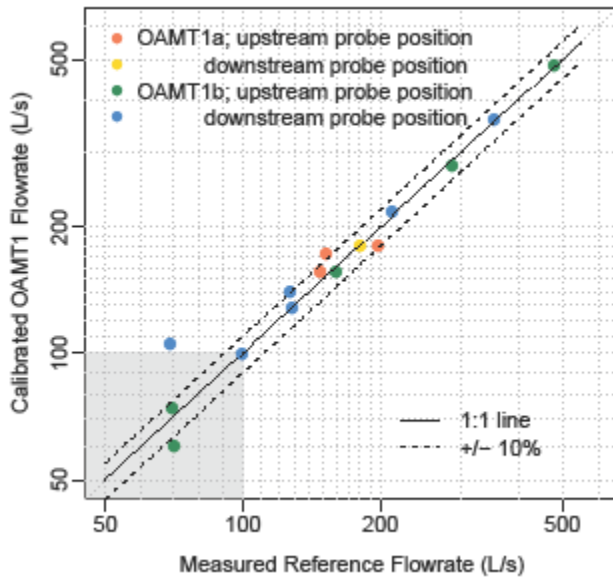


Figure 7. Errors in determination of outdoor air intake flow rates after applying calibration equations.

The prior results depicted in Figures 6 and 7 show the performance of OAMT1a during periods with low wind speeds, usually below 2 m s^{-1} (7.2 km h^{-1}). Figure 8 shows measurement errors of OAMT1a based on rolling 60 minute averages that increase with wind speed when the wind is from the east (75 to 125 degrees). There are no clear trends in error versus wind speed with other wind directions. The maximum winds speeds, except for brief bursts, were only about 4.5 m/s (16.2 km h^{-1}).

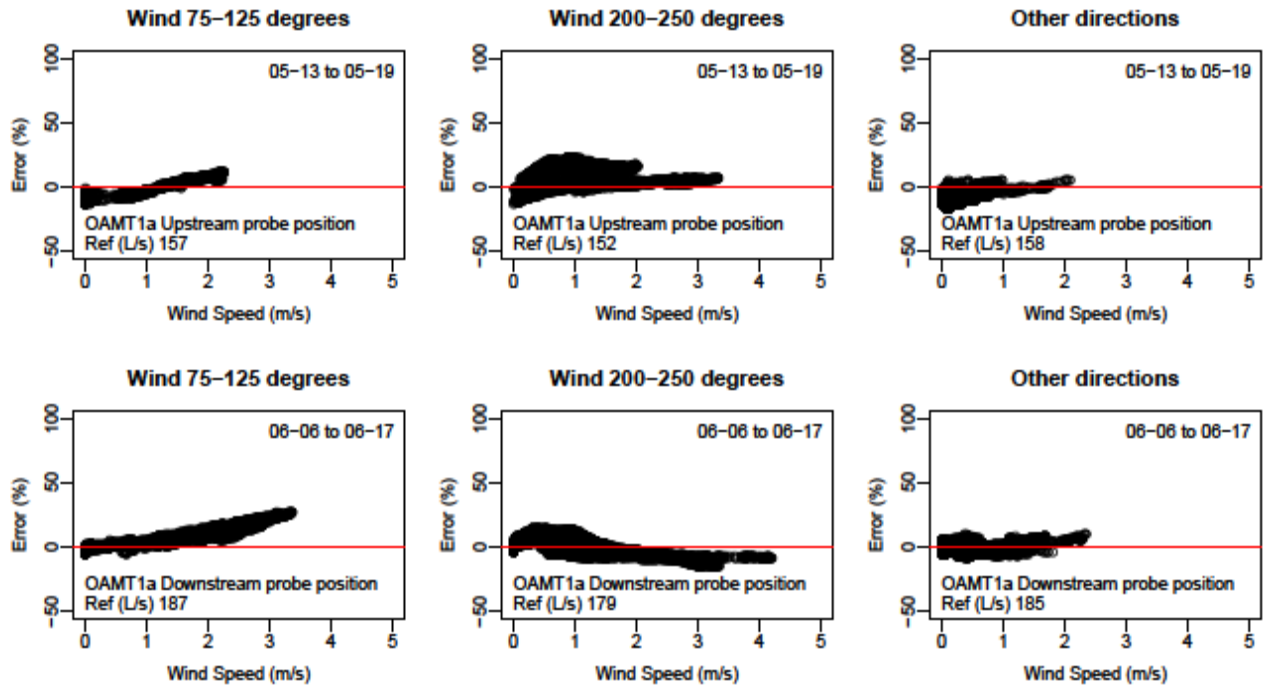


Figure 8. Error in OA intake rates measured with OAMT1a, as a function of wind speed and direction.

The airflow resistance of OAMT1a was based on measurements of the static pressures outside of OAMT1a minus the static pressure inside of OAMT1a at the plane of the velocity probe. The measured airflow resistance was 7 Pa at a flow rate of 580 L s⁻¹, corresponding to an air velocity at the velocity probe of 2 m s⁻¹. At a flow rate of 1,070 L s⁻¹, with corresponding air velocity of 3.7 m s⁻¹, the measured airflow resistance was 19 Pa. A polynomial-based extrapolation to a design maximum flow rate of 1,200 L s⁻¹ (not achievable in the test system) yields an expected maximum airflow resistance of OAMT1a of 24 Pa. These measured values substantially exceed predictions (3.4 Pa 6.7 Pa, 7.6 Pa) of the airflow resistance of the honeycomb airflow straightener based on extrapolation of data provided by the manufacturer of the honeycomb media; however, the measured airflow resistance of OAMT1a easily met the design goal of maintaining the resistance less than 35 Pa.

Table 4 shows the results of a traverse to determine the air velocity profile in the duct downstream of honeycomb airflow straightener, at a location half way between the upstream and downstream probe locations. The outdoor air damper was 25% open. The data indicate substantial variability in air speed confirming, as expected, that the resistance of the airflow straightener is too small to produce a uniform air speed. The low normalized velocities in the right-most column are unexplained, given the symmetry of the upstream airflow path. The low normalized air speeds in the bottom row might be explained by the damper, when 25% open,

having little open area at its base. The data do not explain why OAMT1a, with a velocity probe positioned at the horizontal centerline, indicates an air velocity approximately 40% above the average velocity. Similar results were obtained from a traverse performed with the outdoor air damper 75% open, except the normalized velocities in the final row were closer to unity.

Table 4. Example results of velocity profile in duct section housing probes of OAMT1. Values are speeds normalized by the average speed.

Distance (cm) from: side of duct → top of duct ↓	4.8	18.5	34.4	44.3	60.2	73.9
2.5	1.01	0.96	1.62	1.70	0.67	0.60
10.8	1.55	0.85	1.21	0.97	0.71	0.89
18.4	1.06	0.78	1.52	1.04	0.71	0.96
26.0	0.97	1.06	1.57	2.36	0.94	0.83
34.3	0.98	0.22	0.45	0.50	0.40	0.88

3.2.2 OAMT1b

Figure 9 provides plots of measurement accuracy from tests of OAMT1b during periods with low wind speeds. Results are similar to those of OAMT1a, except that the slopes of the best fit lines are substantially closer to unity, 0.843 and 0.935, indicating the need for a substantially smaller calibration correction with the two-probe system of OAMT1b.

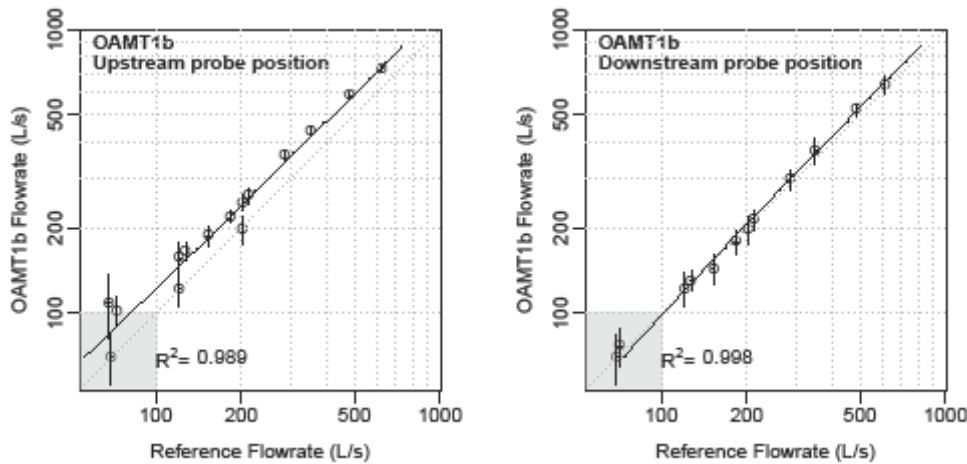


Figure 9. Results of tests of OAMT1b when wind speed are low.

The corrected flow rates from OAMT1b, with the probes in the upstream position can be calculated from the following equation

$$\text{Corrected } F_{1b} = 0.843 F_{1b} - 3.4 \quad (12)$$

With the probes in the downstream position, the corresponding equation is

$$\text{Corrected } F_{1b} = 0.935 F_{1b} + 8.4 \quad (13)$$

Figure 7 shows that errors in determination of OA intake rates with OAMT1b, after applying the calibration equations (equations 12 and 13), are generally within 10%.

Figure 10 shows measurement errors of OAMT1b as a function of wind speed and wind direction based on rolling 60 minute averages of measured data. In one set of data, with a low OA intake rate of 101 L s⁻¹, equal to 8% of the design-maximum flow rate, there is a large and very clear increase in measurement error with wind speed when the wind is from the east (75 to 125 degrees). There are also other sets of data indicating increases or decreases in error with wind speed. The maximum winds speeds, except for brief bursts, were only about 3.5 m/s (12.6 km h⁻¹).

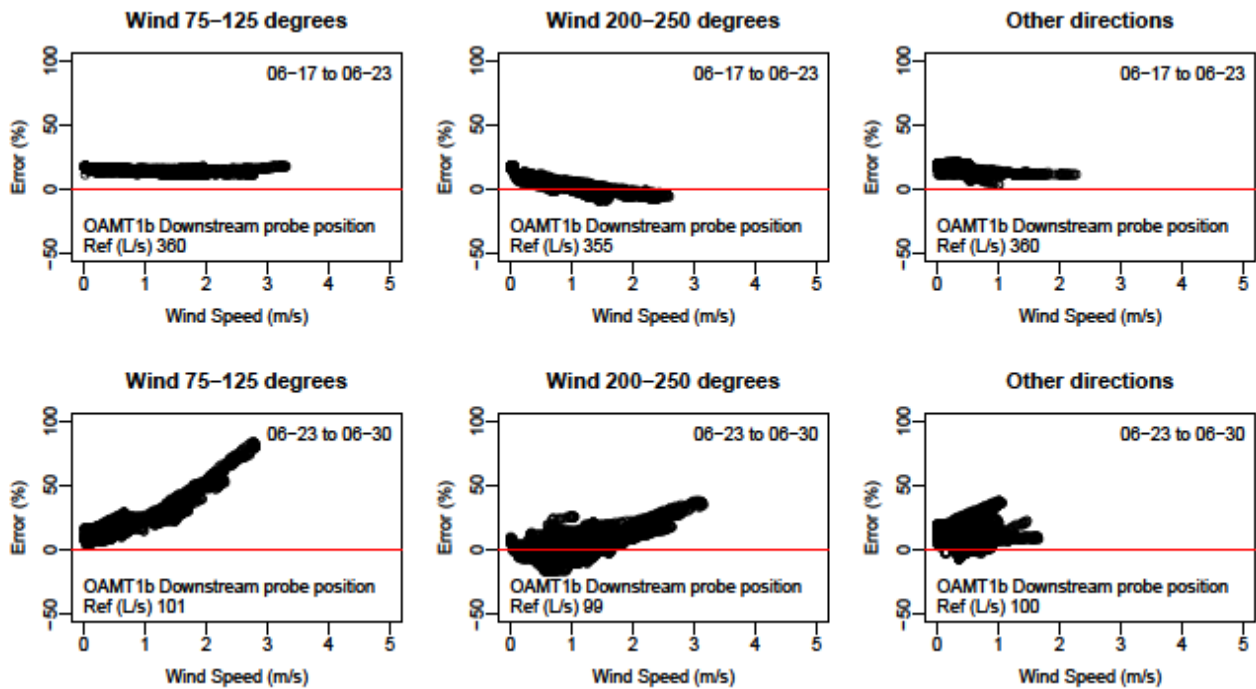


Figure 10. Error in OA intake rates measured with OAMT1b, as a function of wind speed and direction.

OAMT1b differs from OAMT1a only via the substitution of two velocity probes for a single probe. The second probe was not expected to significantly affect airflow resistance, thus, the airflow resistance results for OAMT1a are also assumed applicable to OAMT1b

3.2.3 OAMT1c

Figure 11 provides plots of measurement accuracy from tests of OAMT1c during periods with low wind speeds. The plotted data points are approximately 60 minute averages and in all tests the downstream damper was 75% open. As with OAMT1a and OAMT1b, the airflow rate indicated by the product of air velocity and cross sectional area of the airflow channel, i.e., by equation 7, substantially exceeds the reference airflow rate. The left panel of Figure 11 shows that the data are well fit by a straight line with a non-zero offset indicating that the system could be used to indicate outdoor airflow rate with good accuracy using equation 14.

$$\text{Corrected } F_{1c} = 0.909 F_{1c} - 106 \quad (14)$$

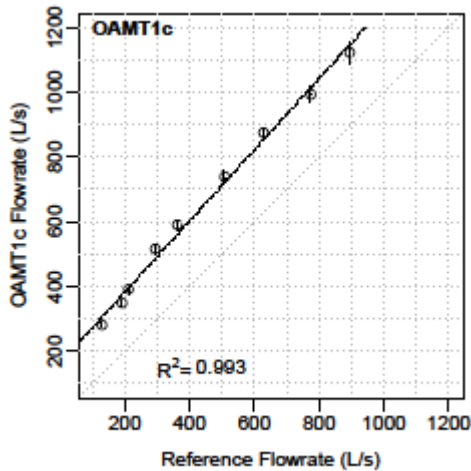


Figure 11. Results of tests of OAMT1c when wind speeds are low.

Figure 12 shows that wind speed and wind direction within the ranges encountered have a small effect on accuracy of OAMT1c.

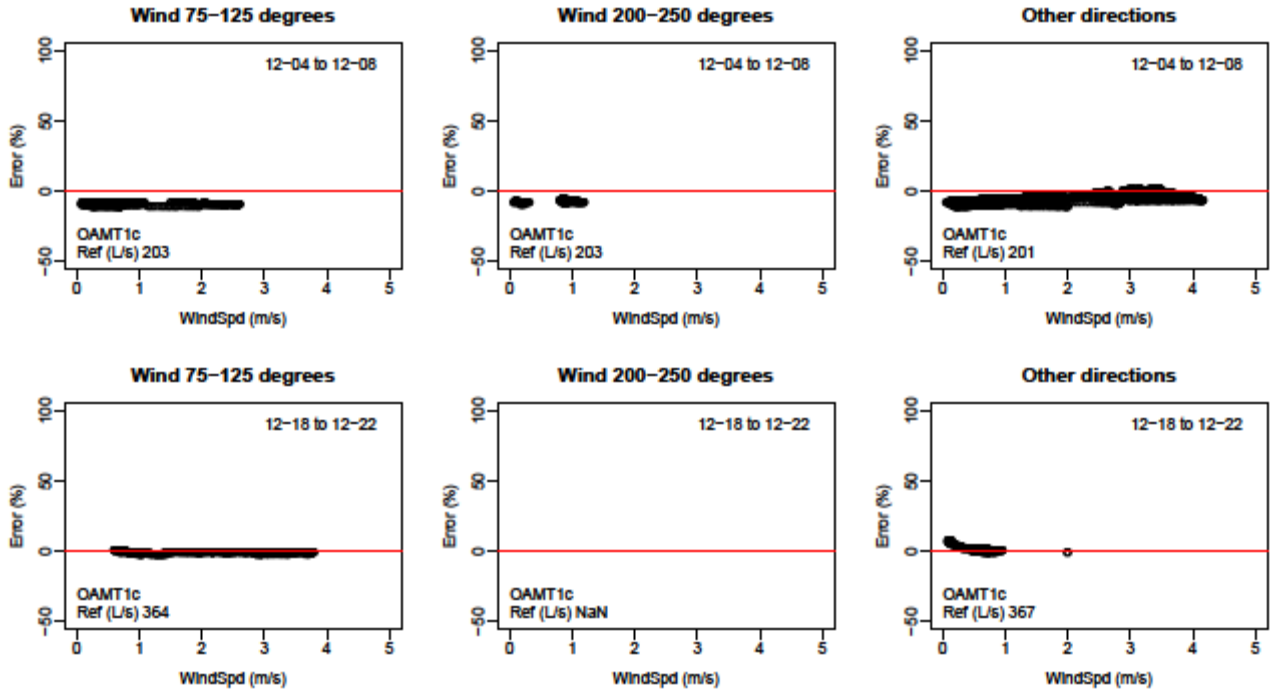


Figure 12. Error in measurements of OA intake rates of OAMT1c versus wind speed and direction, after applying calibration equation 14.

To indicate measurement accuracy using equation 14, the equation was applied to data that were not used for equation generation. The resulting air flow rates are compared to reference values of airflow rate on Figure 13. Nearly all the data points fall within the $\pm 10\%$ confidence band indicating that errors are generally less than 10%.

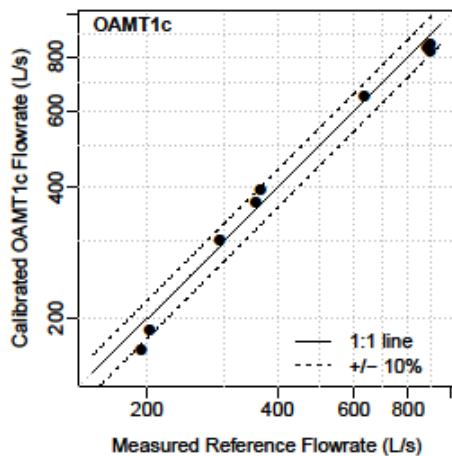


Figure 13. Errors in determination of outdoor air intake flow rates with OAMT1c after applying calibration equation 14.

OAMT1c and OAMT1a use the same velocity probe (Ebtron HTA104PB) centered horizontally in the airflow channel. In both systems, before application of calibration equations, the OAMT system provides an OA intake rate that substantially exceeds the reference airflow rate. To some extent, this discrepancy is expected as centerline air velocities in a rectangular duct will generally exceed the average air velocity. However, a velocity probe that indicates an air velocity higher than the true velocity is another potential partial explanation. A limited check of the accuracy of the velocity probe was performed through use of the hot wire anemometer to measure the air velocity approximately 5 cm upstream of the locations of the four velocity sensors of the probe. This comparison was only performed one time at three OA intake rates. Figure 14 compares the average velocities obtained with the hot wire anemometer and with the velocity probe of OAMT1c, to the average velocity calculated from the reference air flow rate and the cross sectional area of the airflow channel. The velocity measured using the hot wire anemometer more closely matches the air velocity based on the reference air flow. The velocity probe consistently indicates a substantially higher air velocity. This limited comparison suggests a velocity probe that over predicts the true air velocity.

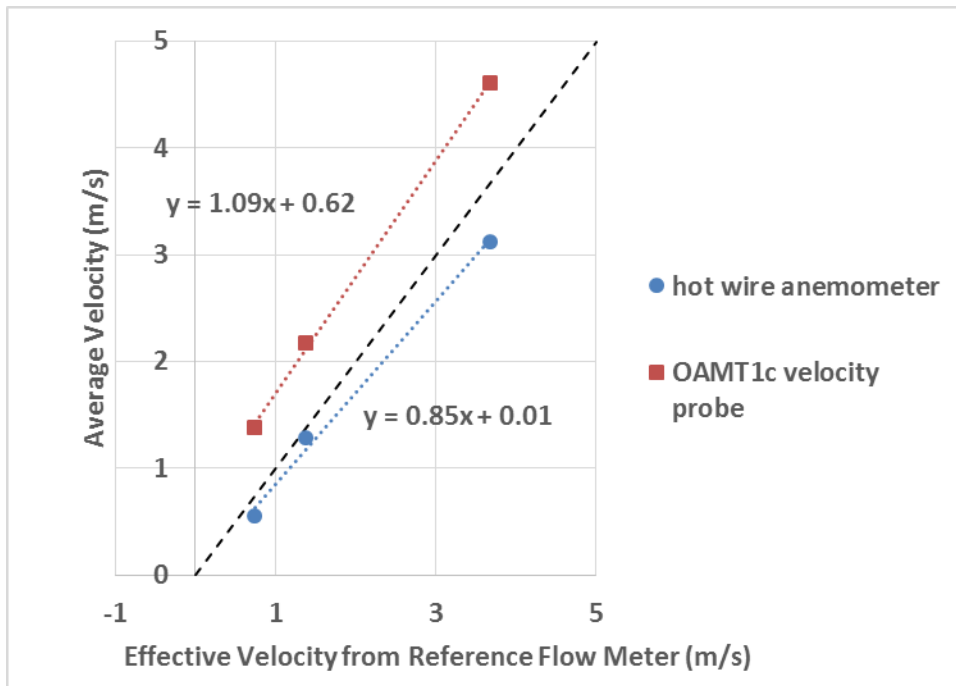


Figure 14. Average air velocities obtained with hot wire anemometer and the velocity probe of OAMT1c compared to the average air velocity based on the reference air flow rate and cross sectional area of the airflow channel.

The airflow resistance of OAMT1c, plus the resistance of the air intake hood, was measured at the maximum achievable airflow rate of 900 L s^{-1} , using the method described for OAMT1a. The result was 23 Pa. Assuming that the airflow resistance increases with velocity squared, the predicted airflow resistance at the system design maximum flow rate of $1,200 \text{ L s}^{-1}$ is 41 Pa. Since the 41 Pa value includes the resistance of the air intake hood, which would be present even without an OAMT, the design appears to have approximately met the targeted maximum airflow resistance of 35 Pa at $1,200 \text{ L s}^{-1}$.

3.2.4 OAMT2

Figure 15 shows the errors in measurements of OA intake rates with OAMT2. Errors are shown with the pressure signal from the velocity probes in OAMT2 measured with the reference pressure transducer (also used in the determination of reference flow rates) and with the less expensive Setra pressure transducer. The Setra transducer, or a similar product, would likely be used in actual OAMT2 systems and with this transducer errors range from -14% to +3%. For flow rates above 100 L s^{-1} , corresponding to above about 8% of the maximum supply air flow rate, errors range from -12% to +3%. Percentage errors diminish and have less spread as flow rates increase. Based on these results, OAMT2 meets the maximum error target of $\pm 20\%$ without incorporation of any calibration factors.

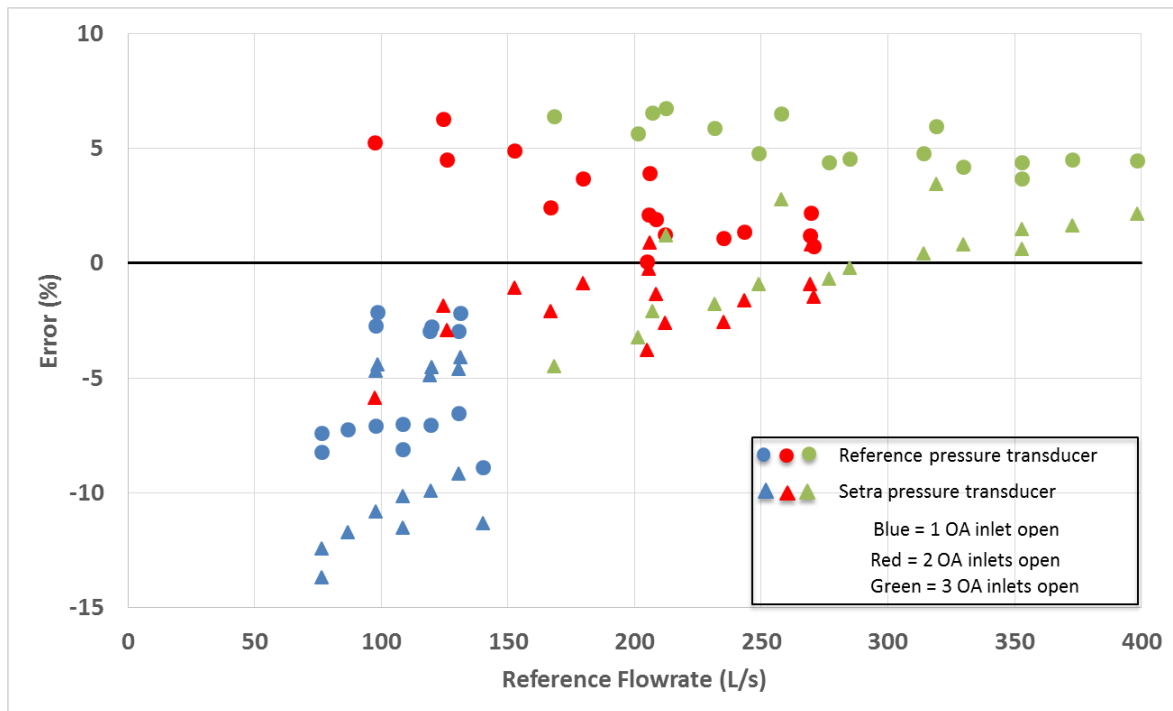


Figure 15. Errors in measurement of OA intake rates with OAMT2, with no application of calibration factors.

Table 5 shows results of linear least square fits to the data from OAMT2. In all cases, data are well fit with R² values of 0.998 to 1.000 and slopes are 0.94 to 1.11. The intercept and slope values could be used to obtain more accurate measurements of OA intake rates, although errors are modest (maximum of 14%) without use of these parameters. Based on the fit parameters, the extent of opening on the OA intake damper had little impact on the performance of OAMT2.

There was no indication that wind speed or direction had a significant influence on the accuracy of OAMT2; thus, accuracy is not shown as a function of wind speed or direction.

Table 5. Linear least square fits to the data from tests of OAMT2.

Pressure Transducer	Open OA Inlets	OA Damper Opening	Intercept	Slope	R ²
Reference	3	75%	-13	0.97	1.000
	3	25%	-16	0.98	1.000
	3	25% & 75%	-14	0.98	1.000
	2	75%	-16	1.02	0.999
	2	25%	-28	1.04	0.999
	2	25% & 75%	-20	1.03	0.999
	1	75%	-3	1.11	1.000
	1	25%	3	1.06	1.000
	1	25% & 75%	-1	1.09	0.998
Setra	3	75%	39	0.94	1.000
	3	25%	38	0.94	1.000
	3	25% & 75%	39	0.94	1.000
	2	75%	10	1.00	0.999
	2	25%	2	1.01	0.998
	2	25% & 75%	8	1.00	0.998
	1	75%	9	1.09	1.000
	1	25%	13	1.05	1.000
	1	25% & 75%	10	1.07	0.997

To indicate measurement accuracy after application of the fitting parameters highlighted in bold in Table 5, “calibrated” OA intake flow rates were calculated for data not used to develop the least square fits. The resulting air flow rates are compared to reference values of airflow rate on Figure 16. All the data points fall well within the ± 10% confidence band indicating that errors are less than 10%. However, the improvement is small, relative to errors with no fitting parameters.

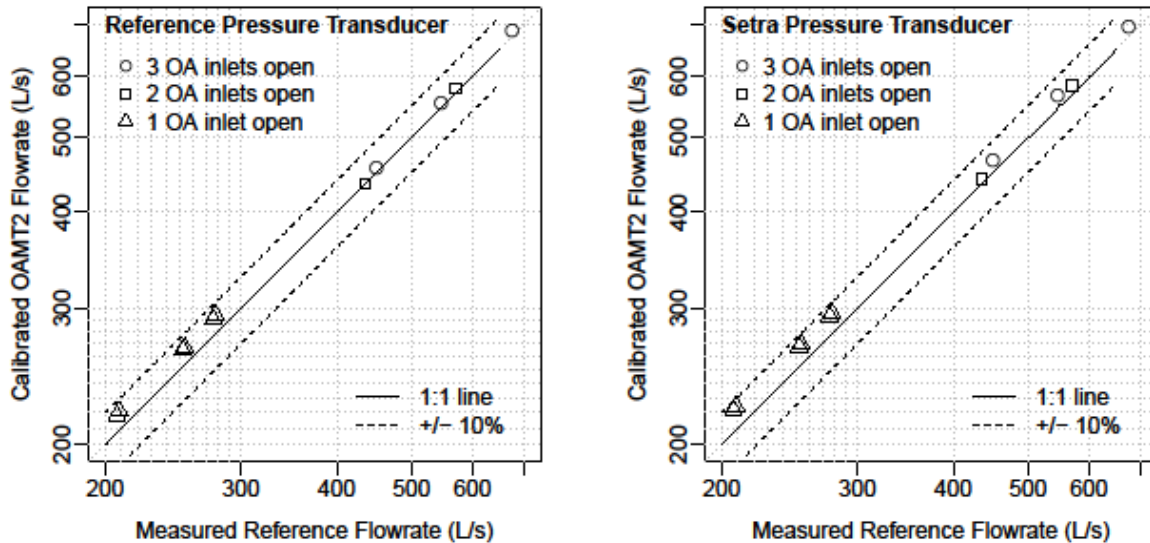


Figure 16. Errors in determination of outdoor air intake flow rates after applying fitting parameters.

The airflow resistance of OAMT2 was measured in conditions simulating a period of economizer operation with a high OA intake rate. During these measurements, the damper within OAMT2 was fully open and two of the OA inlets were open. The airflow resistance was the static pressure outside of OAMT2 minus the static pressure inside OAMT2 downstream of the airflow straighteners. Airflow resistance was 5 Pa at an OA intake flow rate of 532 L s⁻¹ and 21 Pa at 1,053 L s⁻¹, which was the highest flow rate attainable and 89% of the design maximum flow rate for OAMT2 during economizer activation. From a polynomial-based extrapolation, the predicted airflow resistance at the design maximum flow rate of 1,200 L s⁻¹ is 28 Pa, which meets the design target of 35 Pa or less.

4.0 Discussion

This project developed two basic designs for OAMTs applicable to roof top HVAC units. Prototypes of three variants of OAMT1 (OAMT1a, OAMT1b, and OAMT1c) and one variant of OAMT2 were fabricated and tested using a unique roof-top test system. The variants of OAMT1 all used a commercially available electronic air velocity probe (or pair of probes), marketed for measurement of OA intake rates, located downstream of airflow straighteners. OAMT2 employed low cost pressure-based velocity probes downstream of airflow straighteners, plus a damper that increased the air velocity at the probes during periods of minimum OA intake. The

accuracy of measurements of OA intake rates was evaluated as wind speed and direction varied naturally; however, wind speeds were usually 3.5 m s^{-1} (12.6 km h^{-1}) or less.

At low wind speeds, all OAMT systems were able to provide measurements of OA intake rates accurate within approximately $\pm 10\%$ after application of calibration equations; however, OAMT2 met this accuracy target even without application of a calibration equation, except at very low OA intake rates that would be infrequently encountered. When winds speeds exceeded approximately 2 m s^{-1} , with some wind directions the accuracy of OAMT1b was substantially degraded. Wind speed had a more moderate, but still important, adverse effect on the accuracy of OAMT1a. Surprisingly, there was no indication of a significant effect of wind on the accuracy of OAMT1c, which differed from OAMT1a only in the design of the air intake hood and airflow straightener. Wind had no significant effect on the accuracy of OAMT2, possibly because this system uses a damper to increase the air velocity seen by the velocity probes when minimum OA is being provided.

The extent of opening of the OA damper, located downstream of velocity probes, had no clearly discernable effect on measurement accuracy of OAMT1a, OAMT1b, and OAMT2. Tests of OAMT1c were performed only with the damper 75% open.

All prototype OAMT designs had a maximum airflow resistance less than or approximately equal to the targeted maximum of 35 Pa ; thus, all systems would be expected to increase fan energy consumption only marginally.

OAMT1a and OAMT1c, both employed the same electronic air velocity probe and, before application of calibration equations, both systems yielded OA intake rates that substantially exceeded the true or reference value of OA intake. With OAMT1a, the pre-calibration over prediction was approximately 45%. With OAMT1c, data were better fit by an over prediction of approximately 146 L s^{-1} . A limited assessment using a hot wire anemometer suggested that the probe, or probe plus data acquisition system, indicates an air velocity exceeding the true air velocity. Prior to incorporation of a calibration, OAMT1b, which employed two electronic air velocity probes, also over predicted the OA intake rate, but by a much smaller amount, approximately 19% and 7% with upstream and downstream probe locations.

There are performance and cost tradeoffs among the OAMT designs. All of the variants of OAMT1 measure the OA intake rate when minimum OA is supplied and also when an economizer is activated, while OAMT2 only measures the OA intake rate when minimum OA is supplied. In general, it is only important to know the OA intake rate at minimum OA supply conditions; however, the capability of the OAMT1 units to measure OA intake rates when the economizer is activated could indicate faults in economizer systems. OAMT2 provided an accurate measurement of OA intake flow rate without application of a calibration equation, while calibration equations would be needed for all of the variants of OAMT1. Thus, the cost of calibrating is avoided with OAMT2.

The accuracy of OAMT1c and OAMT2 was not significantly affected by wind speed and wind direction, for the ranges encountered, which is an advantage. In fact, the OAMT1a and

OAMT1b designs may be unacceptable due to the effects of wind on accuracy. Changing the unique air intake hood of OAMT1a and OAMT1b to a standard hood, as used in OAMT1c, might reduce the effects of wind on measurement accuracy. Systems costs would also be decreased through use of a more simple air intake hood.

The cost of components varied among the OAMT designs, with the estimated retail component and material costs of prototypes being \$1,318, \$1,663, \$1,298, and \$1,185 for OAMT1a, OAMT1b, OAMT1c, and OAMT2, respectively. Fabrication costs would also vary among units but are not known, as mass production fabrication costs would likely be far lower than the cost of fabricating prototypes in this project. Based on the designs, OAMT1c and OAMT2 would likely have lower fabrication costs than OAMT1a and OAMT1b.

The introduction section described several applications for OAMTs. In most cases, the associated energy savings potential have not been quantified. However, it is known that the energy requirements for ventilation vary widely with climate, building type, HVAC type, and also depend on whether or not the building has an economizer. Benne, Griffith et al. (2009) projected that providing minimum mechanical ventilation in the existing U.S. stock of commercial buildings increased total building energy use by 6.6%, with uncontrolled air infiltration further increasing energy consumption; however, energy impacts varied highly with climate. Overall for the U.S. commercial building stock, gas energy use was much more affected by providing ventilation than electricity use, which suggests that control of MVRs is most critical when heating is needed. However, Benne, Griffith et al. (2009) did not assess how different MVRs, other than no ventilation and the estimated current MVR, influence energy consumption.

The dependence of HVAC energy consumption on different MVRs, ranging from no mechanical ventilation to mechanical ventilation at twice the requirement of Title 24, was modeled using the EnergyPlus program by Dutton and Fisk (2014) and Dutton and Fisk (2015) for offices, a primary school, a secondary school, and a medium-size retail building in California. For the full stock of offices in California, the estimated energy penalty of providing the MVR specified in California Title 24 was approximately 6% of the total HVAC energy use. For California offices with economizers, 50% and 100% increases in Title-24 prescribed MVRs increased HVAC modeled energy use by 7.6% and 21.6%, respectively. In office buildings without economizers, there was a few percent energy savings in many climate zones by increasing VRs up to 150% of the current Title-24-required MVR, because cooling energy savings exceeded heating energy increases by a few percent. In these buildings, increasing the MVR only during periods of cooling would save more energy. In the modeled school buildings, which had no economizers, VRs had only a few percent impact on HVAC energy use. Gas heating energy increased modestly with increased VR and air conditioning energy decreased modestly with increased VR, suggesting a strategy of providing different MVRs during periods of heating and cooling. In the medium-size retail building, projected gas heating energy and total HVAC energy increased markedly with VR, similar to the effects projected for small offices. Total retail building energy use was more moderately affected by VR, for example increasing the VR from

the Title 24 requirement to 150% of the Title 24 requirement was projected to increase total building energy consumption by approximately 7%.

To maximize energy savings using an OAMT, one would modulate MVRs as occupancy and also as weather conditions vary. Features of the building and HVAC system would need to be considered and optimal strategies developed by climate zone. Further analyses are needed to quantify the associated potential energy savings.

5.0 Conclusions

The project designed fabricated and tested prototypes of systems for measuring rates of OA intake into roof top air handlers. All prototypes met the $\pm 20\%$ accuracy target at low wind speeds, with all prototypes accurate within approximately $\pm 10\%$ after application of calibration equations. OAMT2 met the accuracy target without a calibration. With two of four prototypes, OAMT1c and OAMT2, there was no evidence that wind speed or direction affected accuracy; however, winds speeds were generally below usually 3.5 m s^{-1} (12.6 km h^{-1}) and further testing is desirable. The project did not have resources necessary to estimate costs of mass produced systems. The retail cost of components and materials used in the prototypes ranged from \$1,185 to \$1,663. The test data indicate that the basic designs developed in this project, particularly the designs of OAMT1c and OAMT2, have considerable merit. Further design refinement, testing, and cost analysis would be necessary to assess commercial potential. The designs and test results will be communicated to the HVAC manufacturing community after a review of the potential to apply for patents.

6.0 Acknowledgments

This work is supported by the California Energy Commission Public Interest Energy Research Program, Energy-Related Environmental Research Program, award number PIR-12-031 under DOE Contract No. DE-AC02-05CH11231. The authors thank Mary Ann Piette who served as the principal investigator of the broader program of research that incorporated this work and who reviewed a draft of this document. The authors also thank Margarita Kloss for project management, Matthew Fung at the Energy Commission for contract management, and Steve Taylor at Taylor Engineering for engineering advice.

7.0 References

- Arnold, B. D., D. M. Matela and A. C. Veeck (2005). "Life-cycle costing of air filtration." ASHRAE Journal 47(11): 30-32.
- ASHRAE (2013). ANSI/ASHRAE Standard 62.1-2013 Ventilation for acceptable indoor air quality. Atlanta, GA, ASHRAE.
- Benne, K., B. Griffith, N. Long, P. Torcellini, D. Crawley and T. Logee (2009). Assessment of the energy impacts of outside air in the commercial sector, NREL/TP-550-41955. Golden, CO, National Renewable Energy Laboratory.
- Bennett, D. H., W. Fisk, M. G. Apte, X. M. Wu, A. Trout, D. Faulkner and D. Sullivan (2012). "Ventilation, Temperature, and HVAC Characteristics in Small and Medium Commercial Buildings (SMCBs) in California." Indoor Air 22(4): 309-320.
- California Energy Commission (2013). Building energy efficiency standards for residential and nonresidential buildings, Title 24, CEC-400-2012-004-CMF. Sacramento, CA, California Energy Commission.
- Chan, W. R., S. Cohen, M. Sidheswaran, D. Sullivan and W. J. Fisk (2014). "Contaminant levels, source strengths, and ventilation rates in California retail stores." Indoor Air: in press DOI: 10.1111/ina.12152.
- Dutton, S. M. and W. J. Fisk (2014). "Energy and indoor air quality implications of alternative minimum ventilation rates in California offices. ." Building and Environment 82: 121-127.
- Dutton, S. M. and W. J. Fisk (2015). Energy and IAQ implications of alternative minimum ventilation rates in California retail and school buildings. Berkeley, CA, Lawrence Berkeley National Laboratory.
- Fisk, W. J., D. Black and G. Brunner (2011). "Changing ventilation rates in U.S. offices: implications for health, work performance, energy, and associated economics." Building and Environment 47: 368-372.
- Fisk, W. J., D. Faulkner, J. Palonen and O. Seppanen (2002). "Performance and costs of particle air filtration technologies." Indoor Air 12(4): 223-234.
- Fisk, W. J., D. Faulkner and D. P. Sullivan (2005a). "An evaluation of three commercially available technologies for real-time measurement of rates of outdoor airflow into HVAC systems." ASHRAE Transactions 111(2): 443-455.
- Fisk, W. J., D. Faulkner and D. P. Sullivan (2005b). "Technologies for measuring flow rates of outdoor air into HVAC systems: some causes and suggested cures for measurement errors." ASHRAE Transactions 111(2): 456-463.
- Fisk, W. J., D. Faulkner and D. P. Sullivan (2005c). Real-time measurement of rates of outdoor airflow into HVAC systems: a field study of three technologies. LBNL 58856. Berkeley, CA, Lawrence Berkeley National Laboratory.
- Haverinen-Shaughnessy, U., D. J. Moschandreas and R. J. Shaughnessy (2011). "Association between substandard classroom ventilation rates and students' academic achievement." Indoor Air 21(2): 121-131.

Mendell, M. J., E. Eliseeva, M. Spears, W. R. Chan, S. Cohn, D. Sullivan and W. J. Fisk (2014). A prospective study of ventilation rates and illness absence in California office buildings. Berkeley, CA, Lawrence Berkeley National Laboratory.

Mendell, M. J., E. A. Eliseeva, M. M. Davies, M. Spears, A. Lobscheid, W. J. Fisk and M. G. Apte (2013). "Association of classroom ventilation with reduced illness absence: a prospective study in California elementary schools." *Indoor Air* **23**(6): 515-528.

Pacific Northwest National Laboratory (2014). Building component cost community (BC3) database <http://bc3.pnnl.gov/>.

Parthasarathy, S., W. J. Fisk and T. E. McKone (2013). Effect of ventilation on chronic health risks in schools and offices. Berkeley, CA, Lawrence Berkeley National Laboratory. **LBNL-6121E**.

Persily, A. K. and J. Gorfain (2008). Analysis of ventilation data from the U.S. Environmental Protection Agency Building Assessment Survey and Evaluation (BASE) Study, NISTIR-7145-Revised. Bethesda, MD, National Institute for Standards and Technology.

Seppänen, O. A., W. J. Fisk and M. J. Mendell (1999). "Association of ventilation rates and CO₂ concentrations with health and other responses in commercial and institutional buildings." *Indoor Air* **9**(4): 226-252.

Siegel, J. A., J. Srebric, N. Crain, E. Nirlo, M. Zaatari, A. Hoisington, J. Urquidi, S. Shu, Y. S. Kim and D. Jareemit (2012). Ventilation and indoor air quality in retail stores. ASHRAE research project 1596-RP. Atlanta, GA, American Society of Heating, Refrigerating, and Air Conditioning Engineers.

Sundell, J., H. Levin, W. W. Nazaroff, W. S. Cain, W. J. Fisk, D. T. Grimsrud, F. Gyntelberg, Y. Li, A. K. Persily, A. C. Pickering, J. M. Samet, J. D. Spengler, S. T. Taylor and C. J. Weschler (2011). "Ventilation rates and health: multidisciplinary review of the scientific literature." *Indoor Air* **21**(3): 191-204.